

Adaptive gPCA: A method for structured dimensionality reduction

Julia Fukuyama

Department of Statistics, Stanford University

November 14, 2018

Abstract

When working with large biological data sets, exploratory analysis is an important first step for understanding the latent structure and for generating hypotheses to be tested in subsequent analyses. However, when the number of variables is large compared to the number of samples, standard methods such as principal components analysis give results which are unstable and difficult to interpret.

To mitigate these problems, we have developed a method which allows the analyst to incorporate side information about the relationships between the variables in a way that encourages similar variables to have similar loadings on the principal axes. This leads to a low-dimensional representation of the samples which both describes the latent structure and which has axes which are interpretable in terms of groups of closely related variables.

The method is derived by putting a prior encoding the relationships between the variables on the data and following through the analysis on the posterior distributions of the samples. We show that our method does well at reconstructing true latent structure in simulated data and we also demonstrate the method on a dataset investigating the effects of antibiotics on the composition of bacteria in the human gut.

1 Introduction

When analyzing biological data, we are often presented with a large data matrix of interest along with side information about the relationships between the variables in the data set. For example, in microbiome data analysis, we have a data matrix containing abundances of bacterial species as well as information about the phylogenetic relationships between the bacteria. When analyzing transcriptome data, we might have a data matrix with gene expression levels in the various samples as well as information about which pathways the genes are involved in. In light of this, many methods have been developed to perform

statistical analyses while taking into account the structure of the variables. The fused lasso and its variations are often applied to genomic data (Tibshirani and Wang (2008); Tibshirani *et al.* (2005); Rinaldo *et al.* (2009)). Kernel-penalized regression (Randolph *et al.* (2015)) was developed to incorporate phylogenetic structure into regression for microbiome data. The structure encoded by gene networks has also been used to aid in classification of microarray data (Rapaport *et al.* (2007)), and regression analysis of genomic data (Li and Li (2008)).

The current paper presents a new method for exploratory analysis of such data which incorporates information about the relationships between the variables. As motivation for why we might want to include information about the relationships between the variables, consider doing PCA on just the data matrix: we know that PCA is inconsistent when the number of variables is much higher than the number of samples (Johnstone and Lu (2012)), which it usually is in modern datasets. A common solution to the problem of inconsistency is to assume that the principal axes are sparse and estimate them using a regularized version of PCA which encourages sparse principal axes. However, there are situations in which we do not expect sparsity, but do expect other sorts of structure in the data. Our method is designed to perform regularization in these situations.

From a more practical point of view, PCA is undesirable as an exploratory method in situations where we have a large number of variables because the variable loadings on the principal axes are difficult to interpret: first of all, each axis is a linear combination of all the variables, and moreover, the loadings of the variables will not be structured according to our prior knowledge about the relationships between them. Our method ensures that variables which are similar to each other have similar axis loadings. This leads to a more parsimonious explanation of the axes in terms of groups of related variables, which should be more interpretable and biologically relevant. In this regard it has a similar aim as PCA with a fused lasso penalty on the variable loadings (Witten *et al.* (2009)), although it works with more general structures on the variables.

The layout of the paper is as follows: We first introduce a motivating example in which incorporating outside information about the variables is particularly important and which we will later use to illustrate our method. We review generalized PCA, and then show how including a prior in conjunction with the appropriate generalized PCA leads to our new method, adaptive gPCA. To get a better understanding of adaptive gPCA, we show how it is related to existing methods and we demonstrate its performance on simulated and real data.

2 Motivating example

The motivation for this work was our experience analyzing microbiome data. In this paper, we will focus on one particular microbiome data set, first published in Dethlefsen and Relman (2011). The goal of the study was to understand the effect of antibiotics on the composition of bacteria in the human gut. To this end, stool samples were collected from each of three individuals before, during,

and after administration of two courses of the antibiotic Ciprofloxacin. Between 52 and 56 samples were collected from each individual for a total of 162 samples.

To understand what kinds of bacteria were present and at what abundances, a certain highly variable segment of the 16S rRNA gene was amplified by PCR and sequenced using next-generation sequencing. The sequence of the variable segment of this gene was used as a proxy for species. The species defined in this way are known in the microbiome literature as operational taxonomic units (OTUs) and not species since there is not necessarily a direct correspondence between them and previously identified bacterial species. In the original analysis of this data, OTUs were defined by clustering together sequences with at least 95% sequence identity using the Uclust software (Edgar (2010)), and the abundance of each OTU was defined as the number of sequences mapping to the cluster. Clustering sequences with at least 95% sequence identity gave rise to a total of 2582 OTUs.

After defining OTUs in this way, the consensus sequence for each OTU was mapped to a reference phylogenetic tree from the Silva 100 reference database (Quast *et al.* (2013)). This mapping provides us with the phylogenetic relationships between the bacteria corresponding to the sequences that were obtained from the samples.

2.1 The bacterial species problem

No matter how we define OTUs, there is an underlying biological issue in the definition of a bacterial species. Even today, there is a division among microbiologists about whether bacterial species reflect real underlying biology or whether they are primarily for scientists' convenience. On the pro-species side, the "ecotype" theory described in Cohan (2002) gives theoretical justification for why we would expect to see groups of bacteria with much smaller within- than between-group sequence divergence and why these are meaningful biological units. The anti-species side of the debate cites as evidence the large amount of lateral gene transfer and homologous recombination as well as the amount of genetic dissimilarity within groups traditionally defined as species. For an example of this type of argument, see Doolittle and Papke (2006).

However, following Darwin who wrote that "all true classification is genealogical," most microbiologists agree on the usefulness of the phylogenetic tree for describing the relationships between bacteria. For example, Brenner *et al.* (2005), Doolittle and Papke (2006), Cohan (2002), all agree on this despite differing on the existence of bacterial species. Therefore, to bring our statistical methods more in line with biological understanding, methods that deal with bacterial species should incorporate the phylogeny instead of implicitly assuming that species are all equally distinct.

2.2 Existing methods for incorporating phylogeny in microbiome data analysis

Several methods have been proposed for including phylogenetic information in exploratory data analysis. Some examples are double principal coordinates analysis (DPCoA), which was originally described in [Pavoine *et al.* \(2004\)](#) as a method for incorporating more general structure about the variables but which can accommodate phylogenetic structure, weighted and unweighted Unifrac ([Lozupone and Knight \(2005\)](#) and [Lozupone *et al.* \(2007\)](#)) which were developed specifically for microbiome data, a number of variants of the Unifrac distances including generalized Unifrac ([Chen *et al.* \(2012\)](#)) and variance-adjusted weighted Unifrac ([Chang *et al.* \(2011\)](#)), and edge PCA ([Matsen and Evans \(2013\)](#)). Unfortunately, many of these methods tend to implicitly group together species at a very high taxonomic level, which is not always desirable. Although a high-level grouping might lead to good insights in some situations, in general we would like a more flexible method where we can tune how coarse or fine of an analysis to perform.

Another issue with many of the existing methods for incorporating the phylogeny (in particular Unifrac and its variants) is that they are distance-based and when they are applied in conjunction with multi-dimensional scaling they give axes with no interpretation in terms of the species. Since we are interested in dimensionality reduction for hypothesis generation and for understanding the biology underlying the structure we see in the data, it is important for the method to also give insight into which species are responsible for any clustering or gradients we see in the low-dimensional representation of the samples. In contrast to most of the existing methods, the procedure we introduce in this paper will use the phylogenetic relationships between the bacterial species to give interpretations of the axes in terms of groups of closely related species, which we expect to be more easily interpretable and to lead to a better understanding of the differences between microbial communities.

2.3 Other properties of the antibiotic dataset

The data set from [Dethlefsen and Relman \(2011\)](#) that we are considering in this paper also has many of the features we discussed in the introduction. We have 2582 variables (the abundances of the species or OTUs) and only 162 samples, making the variable loadings from PCA difficult to interpret and unreliable. We also do not expect sparsity in the principal axes. The main divisions in the data are samples from different individuals and samples taken during administration of the antibiotic vs. not, and we do not expect either of these divisions to be associated with changes in only a few species. On the contrary, we expect the administration of the antibiotic to change the relative abundances of nearly all of the species, and we know from other microbiome studies that different individuals have very different gut microbiome compositions at the species level (see [Shade and Handelsman \(2012\)](#)). On the other hand, we do expect phylogenetically similar species to react in similar ways to the antibiotic. For all of these

reasons, we expect a method which incorporates the phylogeny to be useful in understanding these data.

3 Generalized PCA

Before we introduce adaptive gPCA, we first review generalized PCA (gPCA) and give some intuition about the kinds of solutions it produces. Generalized PCA has already been used to create structured low-dimensional data representations: For the particular case of analyzing microbiome data with a phylogenetic tree, it was shown that double principal coordinates analysis (Pavoine *et al.* (2004)), which we will look at in more detail later, could be re-expressed as a gPCA (Purdom (2011)). In a rather different context, but also for the purpose of incorporating the structure of the variables into the analysis, the method for functional principal components introduced in Silverman (1996) also has an interpretation as PCA with respect to a non-standard inner product, or a generalized PCA.

We follow the notation from the French multivariate tradition in considering gPCA on a triple (X, Q, D) , where $X \in \mathbb{R}^{n \times p}$ is our data matrix of n samples measured on p variables, and Q and D are positive definite matrices with $Q \in \mathbb{R}^{p \times p}$ and $D \in \mathbb{R}^{n \times n}$ (see Holmes (2008) for a more thorough explanation). The sample scores for gPCA on the triple (X, Q, D) are the solutions to the optimization problem

$$\begin{aligned} \max_{u_i \in \mathbb{R}^n} \quad & u_i^T D X Q X^T D u_i, \quad i = 1, \dots, k \\ \text{s.t.} \quad & u_i^T D u_i = 1, \quad i = 1, \dots, k \\ & u_i^T D u_j = 0, \quad 1 \leq i < j \leq k \end{aligned} \tag{1}$$

Similarly, the principal axes for gPCA on the triple (X, Q, D) are given by

$$\begin{aligned} \max_{v_i \in \mathbb{R}^p} \quad & v_i^T Q X^T D X Q v_i, \quad i = 1, \dots, k \\ \text{s.t.} \quad & v_i^T Q v_i = 1, \quad i = 1, \dots, k \\ & v_i^T Q v_j = 0, \quad 1 \leq i < j \leq k \end{aligned} \tag{2}$$

We can think of gPCA either as PCA in a non-standard inner product space or as PCA on observations corrupted with non-spherical noise. Both ways are informative and we review both here.

3.1 Non-spherical noise

Recall, following Allen *et al.* (2014), that PCA can be formulated as a maximum likelihood problem. Suppose that our observed data is $X \in \mathbb{R}^{n \times p}$, and our model is

$$\begin{aligned} X &= U \Lambda V^T + E \\ E_{ij} &\stackrel{\text{iid}}{\sim} N(0, \sigma^2) \end{aligned}$$

where $U \in \mathbb{R}^{n \times k}$ and $V \in \mathbb{R}^{p \times k}$ are orthogonal, and Λ is diagonal. Then if the row scores, principal axes, and variances of PCA on X are given by $\hat{U} \in \mathbb{R}^{n \times k}$, $\hat{V} \in \mathbb{R}^{p \times k}$, and $\hat{\Lambda} \in \mathbb{R}^{k \times k}$, respectively, then the maximum likelihood estimate of $U\Lambda V^T$ is $\hat{U}\hat{\Lambda}\hat{V}^T$.

The generalized PCA solution is obtained when the elements of the noise matrix E are not independent and identically distributed. If we change our model to

$$X \sim \mathcal{MN}_{n \times p}(U\Lambda V^T, D^{-1}, Q^{-1})$$

and if the row scores, principal axes, and variances of gPCA on the triple (X, Q, D) are given by \hat{U} , \hat{V} , and $\hat{\Lambda}$, then the maximum likelihood estimate of $U\Lambda V^T$ is $\hat{U}\hat{\Lambda}\hat{V}^T$ (Allen *et al.* (2014)). This allows us to account for more complicated error structures: we can have correlation on the rows, on the columns, or both. The error structure is not fully general — it still must be separable — but this formulation allows for some dependence in the noise.

In practice, the assumption of normality of the errors may not be even approximately true if our data is highly skewed or discrete, both of which hold in our motivating example for those bacterial species with low expected counts. In this case, we need to apply some sort of transformation to the raw data so as to bring it more in line with our assumptions. The correct transformation to use will depend on the data in question, but for microbiome count data two common choices are to use a started log transformation or to use the variance-stabilizing transformation from the package DESeq2 (see McMurdie and Holmes (2014) and Callahan *et al.* (2016) for examples and the motivation for this transformation). For the data analyzed in this paper, we transform the counts using a started log transformation and remove some of the bacterial species with particularly large fractions of zero counts.

3.2 Non-standard inner product

The other way of thinking of gPCA on the triple (X, Q, D) is simply as PCA in a non-standard inner product space. Note that Q and D , being positive definite matrices, define inner products on \mathbb{R}^p and \mathbb{R}^n in the following way:

$$\begin{aligned} \langle x, y \rangle_Q &= x^T Q y, & x, y \in \mathbb{R}^p \\ \langle x, y \rangle_D &= x^T D y, & x, y \in \mathbb{R}^n \end{aligned}$$

From the form of the gPCA problem as shown in (1) and (2), we see that gPCA is simply standard PCA with the standard inner product replaced with the Q - and D - inner product for the rows and columns respectively. In particular, gPCA of the triple (X, I, I) is equivalent to standard PCA.

To give some intuition into the reasons for and effects of working in a non-standard inner product space, consider linear discriminant analysis (LDA). In LDA, we have a (centered) data matrix $X \in \mathbb{R}^{n \times p}$, and the samples fall into a set of g groups. Suppose that we have weights for each sample, which are stored

on the diagonal of a matrix $D \in \mathbb{R}^{n \times n}$. Let $Y \in \mathbb{R}^{n \times g}$ be an indicator matrix assigning samples to groups, let $A \in \mathbb{R}^{g \times p}$ be a matrix containing the group means for each of the p variables, let $\Delta_Y = Y^T D Y$ be a matrix containing the group weights, and let the within-group covariance matrix be $W = (X - YA)^T D (X - YA)$.

With this notation, LDA can be written as gPCA on the triple (A, W^{-1}, Δ_Y) . We know that in LDA we want to find a projection that maximizes the ratio of the between-class and the within-class variance. We can think of this as LDA favoring projections in directions of small within-class covariance, or projections along axes v for which $v^T W^{-1} v$ is large. Analogously, if we have a more general gPCA on the triple (X, Q, D) , we can think of the effect of the inner product matrix Q as favoring projections along axes v for which $v^T Q v$ is large.

In LDA, our inner product on the rows comes from the data, but we can also imagine having an inner product on the rows which is based on prior knowledge about the data. In what follows, we will choose an inner product on the rows for which directions where similar variables have similar scores are favored over directions in which similar variables have dissimilar scores.

Remark 1. Note that neither the correlated errors nor the non-standard inner product interpretation of gPCA are entirely satisfactory for the problem we want to solve. In our motivating example, we expect there to be axes which are both smooth on the tree and for which the projections of the samples have a large variance.

From the non-standard inner product interpretation, we know that we can design an inner product on the rows which will pull out axes with these properties. However, there are many ways to construct such inner product matrices and the non-standard inner product interpretation gives us very little insight into which one to choose.

The other interpretation, in which we assume correlated errors, is also not quite right since it assumes structure in the error when we want to encode information about the structure of the signal.

4 Adaptive gPCA

In this section, we describe our proposal for incorporating prior information about the structure of the variables. The basic idea is as follows: We include a prior in our model which encodes our intuition that the variables which are similar to each other should behave in similar ways (in the case of microbiome data the idea is that species close together on the tree will behave similarly). We perform generalized PCA on the posterior estimate of each sample given the data, taking into account the variance structure of the posterior. Varying the scalings of the prior and noise variances gives rise to a one-dimensional family of generalized PCAs which favor progressively smoother solutions according to the structure of the variables. Our method, adaptive gPCA, chooses which member of the family to use by estimating the scalings of the signal and the noise by maximum marginal likelihood.

4.1 Data model

Suppose we have a positive definite similarity matrix $Q \in \mathbb{R}^{p \times p}$ (a kernel matrix) between the variables. To prevent scaling issues, assume that $\text{tr}(Q) = p$. Note that since Q is positive definite, it is also a covariance matrix, and a random vector with covariance Q will have stronger positive correlations between variables which are more similar to each other. For microbiome data with a phylogenetic tree, we will take Q to be the matrix where Q_{ij} represents the amount of shared ancestral branch length between species i and j . We use this kernel matrix for several reasons, one of which is that it is the one implicitly used in DPCoA; it is also related to the covariance of a Brownian motion run along the branches of the tree.

With this in mind, consider the following model for our data matrix X :

$$\mathbf{x}_i \stackrel{\text{iid}}{\sim} N(\mu_i, \sigma_2^2 I), \quad i = 1, \dots, n \quad (3)$$

$$\mu_i \stackrel{\text{iid}}{\sim} N(0, \sigma_1^2 Q), \quad i = 1, \dots, n \quad (4)$$

Here we are simply including a prior in our model. The prior incorporates information about the structure in our variables: since the μ_i 's have covariance equal to a scalar multiple of Q , inference using this prior will allow us to regularize towards this structure, or to smooth the data towards our expectation that similar variables will behave in similar ways.

4.2 PCA on Bayes estimates

We are interested in the “true” values given in μ_i and not the observed data \mathbf{x}_i , and so the appropriate next step is to compute the posterior distribution of the μ_i 's and then perform PCA on these posteriors. We can compute the posterior distribution $\mu_i \mid \mathbf{x}_i$ using Bayes' rule, which is

$$\mu_i \mid \mathbf{x}_i = x \sim N(\sigma_2^{-2} Sx, S) \quad (5)$$

with

$$S = (\sigma_1^{-2} Q^{-1} + \sigma_2^{-2} I)^{-1} \quad (6)$$

Now we want to perform PCA on the posterior estimates of the μ_i 's. We need to take into account the fact that the posterior distributions for each μ_i have non-spherical variance, and so we need to use gPCA instead of standard PCA. The method we use to compute the sample scores and principal axes is described in the following theorem:

Theorem 1. *The row scores from gPCA on the posterior estimates $\mu_i \mid \mathbf{x}_i$ from the model described in Section 4.1 are the same, up to a scaling factor, to the row scores from gPCA on (X, S, I_n) . The principal axes from gPCA on the posterior estimates are the same, up to a scaling factor, as the principal axes from gPCA on (X, S, I_n) pre-multiplied by S .*

Proof. See appendix. □

From this theorem, we see that when we perform gPCA on the posterior estimates obtained from the model described in Section 4.1, different scalings of the prior and the noise variances simply lead to gPCAs with different row inner product matrices.

4.3 A family of gPCAs

Now we can explore the family of inner product matrices which our model gives rise to. Up to a scaling factor, the matrix $S = (\sigma_1^{-2}Q^{-1} + \sigma_2^{-2}I)^{-1}$ depends only on the relative sizes of σ_1 and σ_2 , the scalings for the prior and the noise. We therefore have a one-dimensional family of gPCAs determined by the relative sizes of σ_1 and σ_2 . To get some insight into this family, we can first consider the endpoints.

As $\sigma_1/\sigma_2 \rightarrow 0$, that is, as the noise becomes very small compared to the prior structure, S becomes more and more like a scalar multiple of the identity, and so we approach a scalar multiple of gPCA on the triple (X, I, I) , or standard PCA. At the other end, as $\sigma_2/\sigma_1 \rightarrow 0$, we approach a scalar multiple of gPCA on the triple (X, Q, I) . The gPCA on (X, Q, I) turns out to be very closely related to double principal coordinates analysis (DPCoA, originally described in [Pavoine et al. \(2004\)](#)), which is another method for incorporating information about the variables into the analysis. We will describe DPCoA and its relationship with our method further in Section 5, but for now it suffices to note that this family of gPCAs can be thought of as interpolating between DPCoA and standard PCA or as giving us a tunable parameter controlling how smooth we want the principal axes to be.

We might also wonder why this family is better than other families we might consider. A possibly more natural method would be one where we add a ridge penalty to Q , resulting in gPCA on $(X, Q + \lambda I, I)$. This family has the same endpoints as the family we have described: when $\lambda = 0$ we have gPCA on (X, Q, I) , and as $\lambda \rightarrow \infty$ we get standard PCA. The difference between the two is the path between the two endpoints. Very roughly, when we add a ridge penalty to Q , the main effect is to increase the small eigenvalues, but when we add a ridge penalty to Q^{-1} we make the large eigenvalues more similar to each other. In general, the small eigenvalues of Q correspond to eigenvectors that are very rough (the values are very different for variables which are similar to each other), while the large eigenvalues correspond to eigenvectors that are smooth. When we do structured dimensionality reduction, we are almost always going to want to dampen any variance along rough eigenvectors, but we don't necessarily prefer variance in the direction of an extremely smooth eigenvector over variance in the direction of a mostly-smooth eigenvector. When we use $Q + \lambda I$, we remove the dampening on the rough directions, but when we use $S = (\sigma_1^4 Q^{-1} + \sigma_2^{-2} I)^{-1}$ we keep the eigenvalues of the rough directions small and decrease the difference between eigenvalues of smooth eigenvectors.

4.4 Automatic selection of family member

So far, we have been assuming that σ_1 and σ_2 are known, but this is not generally going to be the case. It is possible to choose values for the two purely subjectively, based on how heavily you want to weight your prior knowledge about the variables compared to the actual data. However, if choosing subjectively is not appealing, the structure of the model suggests that we can estimate the values σ_1 and σ_2 from the data itself by maximum marginal likelihood. To be more concrete, according to our data model we have

$$\mathbf{x}_i \stackrel{\text{iid}}{\sim} N(0, \sigma_1^2 Q + \sigma_2^2 I) \quad (7)$$

The overall log likelihood of the data is therefore (up to a constant factor)

$$\ell(X; \sigma_1, \sigma_2) = -\frac{n}{2} \log |\sigma_1^2 Q + \sigma_2^2 I| - \sum_{i=1}^n \frac{1}{2} \mathbf{x}_i^T (\sigma_1^2 Q + \sigma_2^2 I)^{-1} \mathbf{x}_i \quad (8)$$

Maximizing this likelihood is not a convex problem and there does not appear to be a closed-form solution, but it is possible to transform it into a problem of optimizing one parameter over the unit interval. To do this, we introduce some new notation. Let $r = \sigma_1^2 / (\sigma_1^2 + \sigma_2^2)$, and let $\sigma^2 = \sigma_1^2 + \sigma_2^2$. Let $Q = V \Lambda V^T$ be the eigendecomposition of Q where V is an orthogonal matrix and Λ is diagonal containing the eigenvalues $\lambda_1, \dots, \lambda_p$. Finally, let $\tilde{\mathbf{x}}_i = V^T \mathbf{x}_i$ and \tilde{x}_{ij} be the j th element of $\tilde{\mathbf{x}}_i$. The log likelihood in the new parameterization is

$$\ell(X; r, \sigma) = -\frac{np}{2} \sigma^2 \log |rQ + (1-r)I| - \sigma^{-2} \sum_{i=1}^n \frac{1}{2} \mathbf{x}_i^T (rQ + (1-r)I) \mathbf{x}_i \quad (9)$$

$$= -\frac{np}{2} \sigma^2 \sum_{j=1}^p \log(r\lambda_j + 1 - r) - \sigma^{-2} \sum_{i=1}^n \sum_{j=1}^p \frac{1}{2} \frac{\tilde{x}_{ij}^2}{r\lambda_j + 1 - r} \quad (10)$$

Based on the expression above, we can find a closed-form solution for the maximizing value of σ^2 for any fixed r . This gives us

$$\sigma^{2*}(r) = \frac{1}{np} \sum_{i=1}^n \sum_{j=1}^p \frac{\tilde{x}_{ij}^2}{r\lambda_j + 1 - r} \quad (11)$$

We can then re-write the likelihood as a function of r only. This is still not convex and does not have a closed-form solution, but since we now have only one parameter which lies on the unit interval, the optimization can be performed numerically.

Remark 2. We can get some insight into what sorts of solutions adaptive gPCA will choose by considering some extreme cases. First, consider the case where the covariance of X is equal to Q . In this case, the automatic method will set the noise scaling σ_2 equal to 0, which corresponds to gPCA on (X, I, I) or standard PCA. On the other hand, if the covariance of X is spherical, the prior

or signal scaling will be set equal to zero, corresponding to gPCA on (X, Q, I) . Therefore, when the marginal covariance is already structured according to the prior information on the variables, we don't do any regularization towards the prior structure. On the other hand, when it doesn't seem like the marginal covariance is structured according to the prior information on the variables, we do the maximum amount of regularization towards the prior structure. We can think of this as trying to balance the competing objectives of obtaining a gPCA plot which reflects the directions of maximum variation in the data and one which gives similar variables similar axis loadings.

Remark 3 (Choice of Q). Q can be any positive definite kernel matrix between the variables. A kernel matrix is often a natural way to encode relationships between variables: for example, if the variables are the nodes in a graph, there are many graph kernels available to describe the similarities between the nodes, mostly based on the graph Laplacian. For some examples, see [Kondor and Lafferty \(2002\)](#).

If we start off with Euclidean distances between variables instead of similarities, a natural way to create a kernel matrix is as follows: Suppose $\delta \in \mathbb{R}^{p \times p}$ is a matrix with the squared distances between the variables, and let $P = I - \mathbf{1}_p \mathbf{1}_p^T / p$ be the centering matrix. Then, if the distances implied by δ are Euclidean, $-P\delta P$ is a positive definite similarity matrix. This matrix contains the inner products between points if they are embedded in \mathbb{R}^p such that the distances between them match the distances implied by δ and they are centered around the origin.

4.5 Adaptive gPCA

Putting everything together, we have the following method. We start out with a data matrix $X \in \mathbb{R}^{n \times p}$ and either a kernel matrix $Q \in \mathbb{R}^{p \times p}$ containing similarities between the variables or a matrix $\delta \in \mathbb{R}^{p \times p}$ containing the squared distances between the variables (we assume the set of distances is Euclidean). We perform the following steps:

1. If we started with distances between the variables, set $Q = P(-\delta/2)P$. Since the distances are Euclidean, this definition of Q gives a positive definite kernel matrix. Otherwise use the kernel matrix provided.
2. Find σ_1 and σ_2 which maximize the likelihood function in equation (8) corresponding to the model in (4)-(3).
3. Let $S = (\sigma_1^{-2}Q^{-1} + \sigma_2^{-2}I)^{-1}$. Perform gPCA on the triple (X, S, I) . The sample scores for adaptive gPCA are given by the row scores of this gPCA, and the variable scores for adaptive gPCA are given by the column scores of this gPCA pre-multiplied by S .

To understand why this method encourages principal axes with variable loadings which are similar for variables which are similar to each other, recall the description in Section 3.2 of LDA as a gPCA on (A, W^{-1}, D) (where A

is a matrix of group means, W is the within-class covariance matrix, and D is a diagonal weight matrix). The interpretation here is that the discriminant vectors v are encouraged to be in directions where the within-class covariance is small, or $v^T W^{-1} v$ is large. Similarly, gPCA on (X, S, I) will encourage principal axes v for which $v^T S v$ is large. Since S has the same eigenvectors with the same ordering of eigenvalues as Q , the similarity matrix for the variables, this is the same as encouraging principal axes v which have similar loadings for variables which are similar to each other.

5 Relationship with DPCoA

The family of gPCAs given by our method can be thought of as bridging the gap between standard PCA and another method for incorporating information on the structure of the variables, double principal coordinates analysis (DPCoA), originally described in [Pavoine *et al.* \(2004\)](#). Briefly, DPCoA is a method for giving a low-dimensional representation of ecological count data (generally the abundance of species at several sampling sites) taking into account information about the similarities between species. DPCoA starts with a matrix of Euclidean distances between the species and the counts of each species at each sampling site. To obtain the DPCoA ordination, we perform the following steps:

1. Perform a full multi-dimensional scaling on the species.
2. Place each sampling site at the center of mass of the species vector corresponding to that site.
3. Perform PCA on the matrix of sampling site coordinates, and project both the sampling site points and the species points onto the PCA axes.

DPCoA was later shown to be equivalent to gPCA using a certain non-standard inner product in [Purdum \(2011\)](#) for the special case of tree-structured variables, and it can be shown to be equivalent to a gPCA given any Euclidean distance structure on the variables. The relationship between DPCoA with Euclidean distances between the variables and gPCA is given in the following theorem.

Theorem 2. *Suppose we have a count matrix $X \in \mathbb{R}^{n \times p}$ and a set of Euclidean distances between the p variables. We construct a matrix $\delta \in \mathbb{R}^{p \times p}$ containing the squares of the distances between the variables. Let $w_L = X\mathbf{1}/\mathbf{1}^T X\mathbf{1}$, $w_S = X^T \mathbf{1}/\mathbf{1}^T X\mathbf{1}$, and for any weight vector w let $P_w = I - \mathbf{1}w^T$ and D_w denote the diagonal matrix with w on the diagonal. Then:*

1. *The row scores from DPCoA on X using the distances implied by δ are the same (up to a sign change) as the row scores obtained from gPCA on $(D_{w_L}^{-1} X P_{w_S}, P_{w_S}(-\delta/2) P_{w_S}, D_{w_L})$.*
2. *If the column scores from gPCA on $(D_{w_L}^{-1} X P_{w_S}, P_{w_S}(-\delta/2) P_{w_S}, D_{w_L})$ are given by Z , then the column scores from DPCoA on X using the distances implied by δ are the same (up to a sign change) as $P_{w_S}(-\delta/2) P_{w_S} Z$.*

Proof. See the appendix. □

DPCoA was developed for count data, and in the French multivariate tradition count data is typically analyzed by transforming the counts into relative abundances and retaining the column and row sums as weightings on the rows and columns (see, for example, the section on correspondence analysis in [Holmes \(2008\)](#)). The row and column sums need to be retained and used as weights since they give the precision with which we know the relative abundance vectors for each location. Therefore, in the gPCA formulation of DPCoA, we use centering matrices which are weighted according to the variable weights (P_{w_S}) and use an inner product on the columns which weights the rows according to their counts (D_{w_L}). However, with the more general kinds of data we are considering in this paper, we will not necessarily have a measure of the precision with which the variables are measured, and the natural adaptation of the method to non-count data would be to weight all the variables equally. This means setting $w_S = \mathbf{1}/p$ and $w_L = \mathbf{1}/n$. In this case, the gPCA triple becomes $(XP, P(-\delta/2)P, I)$ (with $P = I - \mathbf{1}\mathbf{1}^T/p$, a centering matrix). The inner product matrix here is the limiting inner product matrix in our family of gPCAs as $\sigma_2/\sigma_1 \rightarrow 0$, and the data matrix is simply a standard centered data matrix. Thus, we see that a small modification of DPCoA adapting it to non-count data is equivalent to one of the endpoints in our family of gPCAs.

6 Simulation results

To evaluate the performance of adaptive gPCA, we simulated data from models in which we would hope for it to perform well. To match our motivating example of microbiome abundance data with information about the phylogenetic relationships between the bacteria, we suppose that the variables are related to each other by a phylogenetic tree. We used a random tree (using the function `rtree` in the `ape` package [Paradis *et al.* \(2004\)](#) in R) for the relationship between the variables, and the similarity matrix $Q \in \mathbb{R}^{p \times p}$ we use to encode the information about the tree structure is defined as follows:

$$Q = \mathbf{1}s^T + s\mathbf{1}^T - \delta \tag{12}$$

where $s \in \mathbb{R}^p$ gives the distance between each leaf node and the root and $\delta \in \mathbb{R}^{p \times p}$ gives the distance on the tree between the leaf nodes. This definition gives us a matrix Q with Q_{ij} proportional to the amount of shared ancestry between nodes i and j , and it is also equal to the covariance matrix of a Brownian motion on the phylogenetic tree. For our two simulation experiments, we will compare adaptive gPCA using Q as the similarity matrix to standard PCA and gPCA on (X, Q, I) , which is intended to be a slight extension of DPCoA to real-valued data.

6.1 Simulation A

For the first simulation, we generate our data matrix as rank-one plus noise, and we ensure that the coefficients of the principal axis are smooth on the tree. More specifically, we generate our data matrix $X \in \mathbb{R}^{n \times p}$ as follows:

$$X = uv^T + E \quad (13)$$

$$E_{ij} \stackrel{\text{i.i.d.}}{\sim} N(0, \sigma^2), \quad i = 1, \dots, n, j = 1, \dots, p \quad (14)$$

$$u_i \stackrel{\text{i.i.d.}}{\sim} N(0, 1), \quad i = 1, \dots, n \quad (15)$$

$$v \sim N(\mathbf{0}_p, V_{(m)}V_{(m)}^T) \quad (16)$$

where $V_{(m)} \in \mathbb{R}^{p \times m}$ denotes the matrix whose columns are the top m eigenvectors of Q . The value of m governs how smooth v is: if m is small, v tends to have coefficients which are very smooth and exhibit long-range positive dependence on the tree, and as m increases the coefficients get more and more rough. At the extreme case of $m = p$, $V_{(m)}V_{(m)}^T = I_p$, and so there is no relationship at all between the coefficients of v and the tree structure.

We compare adaptive gPCA to standard PCA and gPCA on (X, Q, I) (intended to be similar to DPCoA), looking at the correlations between the true and estimated scores and principal axes. We vary both m (controlling the smoothness of the principal axis on the tree) and σ the error noise. The results are shown in Figure 1. We see that both standard PCA and adaptive gPCA do a perfect job at recovering both the principal axis and the scores when there is no noise, while gPCA on (X, Q, I) does poorly at recovering the principal axis unless there is very strong long-range dependence in the coefficients of the principal axis (corresponding to $m = 1$ in the left-most column). The performance of all the methods degrades with increasing noise, but the performance of adaptive gPCA falls off less quickly than the performance of PCA when there is at least a moderate amount of smoothness in the coefficients of the principal axis.

6.2 Simulation B

The second simulation is similar to the first, with the difference being how the principal axis is generated. Our data matrix X is again simulated as rank one plus noise, and X , E , and u follow the relations on lines (14), (15), and (16). The difference is in how we create the principal axis. For any branch b in the phylogenetic tree, let $\mathbf{I}_b \in \mathbb{R}^p$ be the indicator vector of the leaf nodes which descend from b . Our principal axes v are then defined as

$$v = \mathbf{I}_b / \sqrt{\mathbf{I}_b^T \mathbf{1}} \quad (17)$$

We generated data matrices X according to this scheme, varying both σ (the variance of the noise term) and b . We did one simulation for each branch b which has between 50 and 200 leaf nodes as descendants. As before, we computed the

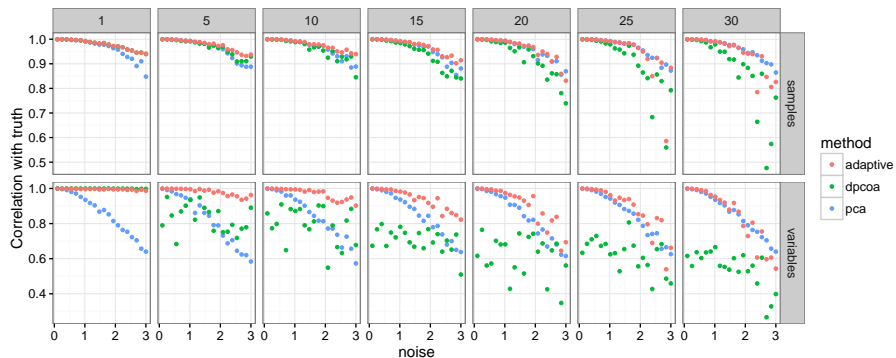


Figure 1: Results from simulation A. Correlations between the true and estimated principal axis (top) and true and estimated scores (bottom) for different values of m (columns, see text for explanation of m).

correlation between the true and estimated principal axis and the true and estimated sample scores along the principal axis, and the results are shown in Figure 2. In this simulation, we see that gPCA on (X, Q, I) does the best when the number of leaf nodes associated with the principal axis is high. Adaptive gPCA consistently outperforms both gPCA on (X, Q, I) and standard PCA in this setup, with the performance not dropping off as quickly as standard PCA does in the presence of increasing amounts of noise.

In both of these simulations, the principal axes are structured according to the tree in some sense, but in neither case is the data generated according to the exact data model described in Section 4.1. This suggests that the method is not overly dependent on the data coming from the exact model which was used to motivate it and can perform well in a variety of situations.

7 Real data example

To illustrate the method on real data, we return to the data set described in Section 2. To review, the goal of the study was to understand the effect of antibiotics on the gut microbiome, and to this end fecal samples were taken from three subjects over the course of several months, during which time each of the subjects took two courses of the antibiotic Ciprofloxacin. Bacterial abundances in the fecal samples were measured using the procedure described in Section 2. Measurements were made before the first course of Cipro (called Pre Cp), during the first course of antibiotics (1st Cp), in the week after the first course of antibiotics (1st WPC), more than one week after the first course of antibiotics and before the second course (Interim), during the second course of antibiotics (2nd Cp), in the first week after the second course of antibiotics (2nd WPC), and after that (Post Cp). For each of the samples we have the abundances of approximately 2000 bacterial species and a tree describing the phylogenetic

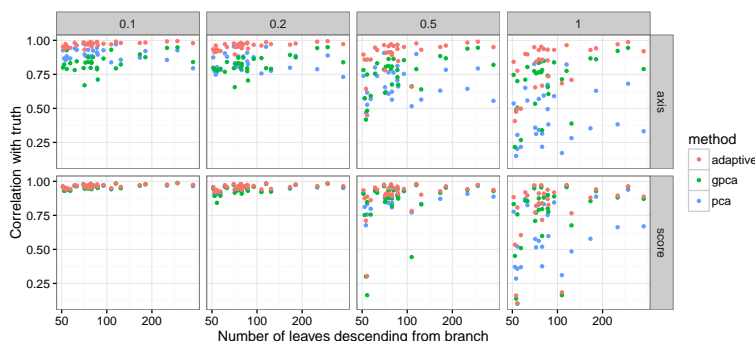


Figure 2: Results from simulation B. Correlations between the true and estimated principal axis (top) and the true and estimated scores along the principal axis (bottom) for different levels of noise variance (columns labeled by noise variance). For each simulation, the principal axis is non-zero on all the leaves descending from a certain branch in the tree, and the x -axis gives the number of non-zero elements.

relationships between the bacteria. We looked at the results from adaptive gPCA, DPCoA, and standard PCA on this data set. In adaptive gPCA, the similarity matrix Q used to incorporate the phylogeny is formed in the same way as for the simulations (see equation (12)) so that Q_{ij} gives the amount of shared ancestry between species i and j .

Figure 3 shows the results of using the three methods on this data set. The top pair of plots shows the results from DPCoA, the middle from adaptive gPCA, and the bottom from standard PCA. In each pair, the left-hand plot shows the sample scores on the first and second principal axes, and the right-hand plot shows the variable loadings on the first and second principal axes. All the pairs of plots can be interpreted as biplots, so if a sample has a large score on e.g. the first principal axis, we expect it to have larger values for variables which have large loadings on the first principal axis.

The three methods give us quite different results. Just considering the sample points to start with, in the DPCoA representation we see some difference in the samples taken while the subjects were on antibiotics compared with the others, but we see very little difference between samples from the different subjects. PCA and adaptive gPCA show complete separation between the samples from the different subjects and a good degree of offset between the samples taken while the subjects were on antibiotics compared with the rest. It turns out that the second adaptive gPCA axis describes the antibiotic perturbation very well: if we plot the scores along the second axis over time, we see that the scores are stable when the subjects are not on antibiotics, drop upon administration of the antibiotic, and return to baseline when the antibiotic is stopped (see Figure 4).

Turning next to the variable (species) loadings on the principal axes, we see

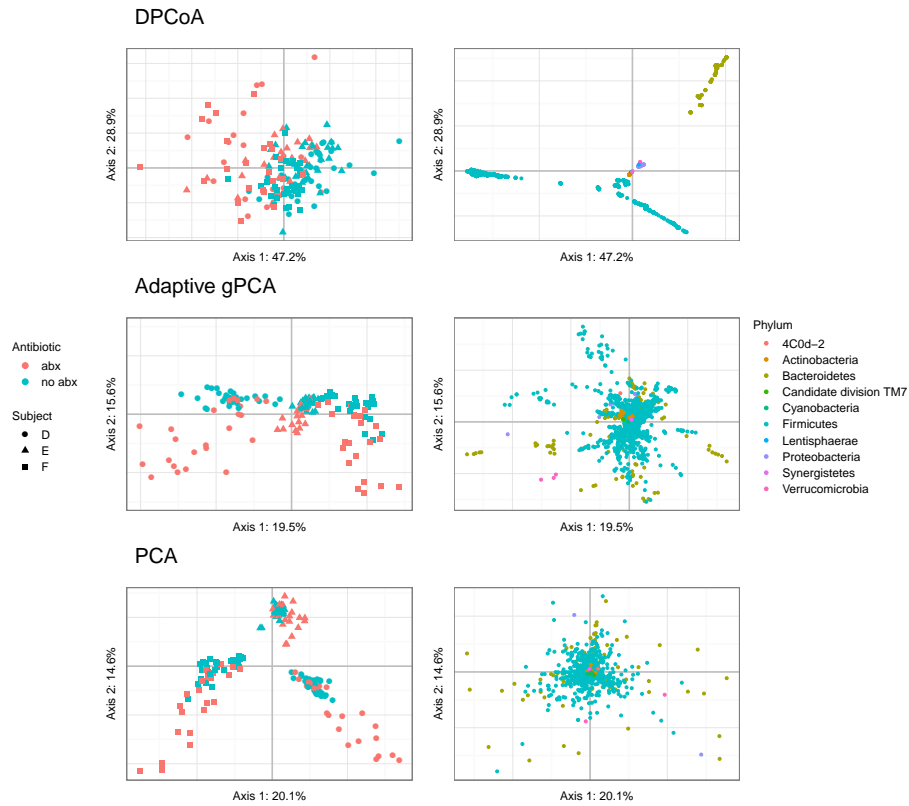


Figure 3: Sample (left) and species (right) plots for DPCoA (top), adaptive gPCA (middle), and standard PCA (bottom). Colors in the sample plots represent a binning of the sample points into abx (either when the subject was on antibiotics or the week immediately after) or no abx (all other times). The colors in the species plots represent phyla.

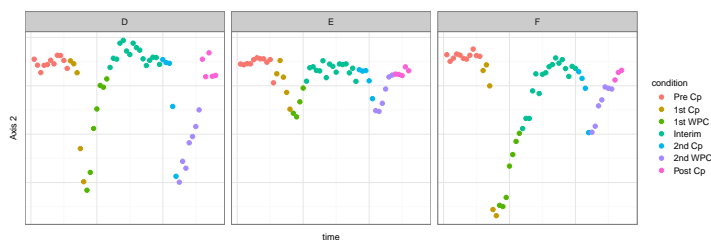


Figure 4: A plot of the scores along the second axis from adaptive gPCA by time, plotted for each of the three individuals. We see very clearly that this axis is capturing species that change during the administration of the antibiotic but which are stable otherwise. The corresponding plots for PCA and DPCoA are much less compelling.

that the species points from PCA show no association with the tree: species which are similar phylogenetically are no more likely to have similar loadings on the principal axes than species which are phylogenetically dissimilar. On the other end of the spectrum, the species points from DPCoA are very related to the tree, and in particular have loadings which are related to the deep branching structure of the tree. We see this in the fact that the species points from the two dominant phyla occupy completely disjoint areas in the variable space. Adaptive gPCA gives results somewhere in the middle: we see that species which are phylogenetically similar are more likely to have similar loadings on the principal axes, but the phenomenon is more local. Whereas in DPCoA, we have very large groups of similar species with similar loadings on the principal axes (the two large phyla), in adaptive gPCA we get smaller groups of similar species having similar loadings on the principal axes.

Since the purpose of the study was to understand the effect of antibiotics on the gut microbiome and since the second adaptive gPCA axis seems to describe the disturbance due to the antibiotic, we can look in more detail at the behavior of the species with large positive or negative loadings on the second adaptive gPCA axis. The 27 species with the largest positive scores along the second adaptive gPCA axis are all of the genus *Faecalibacterium* (and in fact there are 28 members of this genus represented in the data set so this is nearly the entire genus). Although different members of the genus are present or absent in different subjects, when present they all show the same pattern of declining in relative abundance during the treatment with antibiotics and rebounding when the treatment is discontinued. This is shown in the top row of Figure 5. Consistent with what we see in Figure 4, Subject E shows much less of a disturbance compared to subjects D and F, and the disturbance in F corresponding to the second course of antibiotics is much smaller than that corresponding to the first.

Similarly, if we look at the 21 members of the Firmicutes phylum with the largest negative scores along the second adaptive gPCA axis, we see a similar

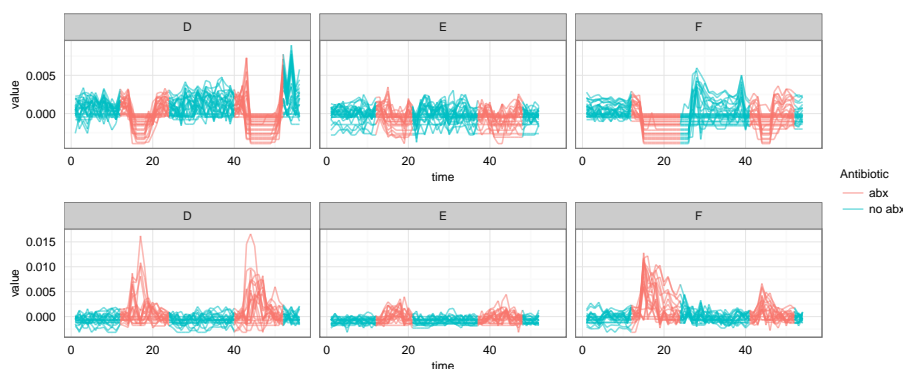


Figure 5: Normalized abundances for two groups of species. Each line represents a species, each facet represents a subject. The top row shows the normalized abundances of each of 27 OTUs with the largest positive loadings on the second adaptive gPCA axis, and the bottom row shows the normalized abundances of the 21 Firmicutes with the largest negative loadings on the second adaptive gPCA axis. In general, the species with positive scores on the second axis see their relative abundances decline with the antibiotic treatment while the species with negative scores see their relative abundances increase. The sizes of the disturbances are consistent with what we see in Figure 4 (e.g. E has the smallest disturbance and the second antibiotic treatment for F leads to a smaller disturbance than the first).

phenomenon. Only 11 of the 21 species in this group are classified at the genus level, but those 11 are all classified as *Blautia*, and all 21 species are classified at the family level as Lachnospiraceae. These species tend to be even more subject specific than those discussed above, with each species usually present in large numbers in only one subject. However, when a species in this group is present in a subject, its relative abundance tends to increase when the antibiotic is administered and falls back to baseline when the treatment is discontinued (shown in the bottom row of Figure 5). This shows us another advantage of using a method which incorporates phylogenetic information: Instead of having a long list of species which may only be present in one subject and whose behavior may not generalize to other individuals, we have a clade whose members, when present, increase in relative abundance with the administration of Cipro. This is a much more parsimonious conclusion than that drawn from a list of unrelated taxa, and it is straightforward to reason about and to test in later experiments.

The results of this analysis show us some of the drawbacks of DPCoA and standard PCA compared with adaptive gPCA. With standard PCA the axes are difficult to interpret because of the lack of relationship between the phylogenetic structure and the loadings of the variables on the principal axes. DPCoA misses much of the true latent structure in the data (it shows almost no subject effect and a smaller antibiotic effect than either adaptive gPCA or standard PCA),

which is consistent with the simulations showing that DPCoA only performs well in very limited situations. Adaptive gPCA recovers the latent structure well and also has axes which are interpretable in terms of small groups of related species. This sort of structure is useful to scientists interested in understanding the underlying biology, and looking in more detail at the groups of species associated with the axes can give us insight into this biology and ideas about what steps to take next.

8 Conclusion

In this paper, we have presented a method for creating low-dimensional representations of a data matrix while taking into account side information about the relationships between the variables. This is done in a natural way by using a prior encoding the relationships between the variables and performing PCA on the resulting posteriors, taking into account the fact that the posteriors have non-spherical variance. We show that performing PCA on the posterior estimates obtained with this prior corresponds to a generalized PCA, with a one-dimensional family of gPCAs arising from varying the prior strength. A member of this family can then be picked by estimating the scalings of the prior and the noise by maximum marginal likelihood. We call the gPCA obtained in this manner adaptive gPCA.

Adaptive gPCA leads to a low-dimensional representation of the samples. The loadings of similar variables along the principal axes in this representation will be similar to each other, allowing the axes to be more interpretable than in standard PCA. The effect is therefore similar to what we would obtain by using PCA with a fused lasso penalty on the variable loadings, but the motivation and derivation are different, and our method is able to accommodate more general variable structures than the fused lasso. Other attractive features of our method are that we can obtain the global solution without worrying about the algorithm being stuck in a local minimum and that we can choose the amount of regularization to perform without having to resort to potentially time-consuming cross-validation.

Using adaptive gPCA on a real data set shows us some of the advantages of the method: we were able to identify the latent structure in the data (the differences between the individuals and the antibiotic treatment), and we were able to use the loadings of the variables on the principal axes to understand the biology behind this latent structure. For instance, the second adaptive gPCA axis was related to the administration of the antibiotic, and examining the loadings of the species along the second axis gave us groups of closely-related species which share the same behavior upon administration of the antibiotic. The implicit smoothing done by adaptive gPCA is helpful here because not all the members of each group of species identified by adaptive gPCA are present in each sample, but nonetheless the members of the groups have similar behaviors when they are present.

It is also possible to extend adaptive gPCA in a number of directions. If we

have information about the precision with which different variables or samples are measured, it is easy to incorporate either sample or variable weights into the analysis. The family of inner products described in this paper can also be used with other methods which work in non-standard inner product spaces, such as between- or within-class analysis (Dray *et al.* (2015)), to encourage loading vectors which are smooth according to the structure of the variables. It can also be used in conjunction with formulations for sparse gPCA (Allen *et al.* (2014)) to obtain low-dimensional representations of the variables which are both sparse and structured, and combining this further with between-class analysis would yield a method for supervised learning with sparse and structured variable loadings.

An R implementation of adaptive gPCA is available at

www.github.com/jfukuyama/adaptiveGPCA

and can be installed in R with the command

```
devtools::install_github("jfukuyama/adaptiveGPCA")
```

The package allows for either the automatic selection procedure described in Section 4 or for manual selection. Manual selection is mediated by a shiny gadget Chang *et al.* (2016), which provides an interactive plot with a slider bar allowing the user to move easily between visualizations corresponding to different prior strengths. The package also includes the antibiotic data used in this paper and a vignette which reproduces the analysis.

A Proof of Theorem 1

The posterior distribution of all of the μ_i 's given the data follows a matrix normal distribution $\mathcal{MN}_{n \times p}(\sigma_2^{-2}XS, I_n, S)$. Therefore, following the structured error interpretation of gPCA, to take into account the error structure we should perform gPCA on the triple $(\sigma_2^{-2}XS, S^{-1}, I_n)$. Since we are interested in the low-dimensional representation of the samples and variables, the scaling is not important and going forward we will drop the σ_2^{-2} factor and consider gPCA on (XS, S^{-1}, I_n) .

Now, note that the sample scores obtained by gPCA on (XS, S^{-1}, I_n) are the same as those obtained by gPCA on (X, S, I_n) , as can be verified by plugging both sets of variables into the optimization problem in (1). The principal axes from (XS, S^{-1}, I_n) are equal to the principal axes from (X, S, I_n) transformed by S . To see the equivalence, note that for the principal axes from the triple (XS, S^{-1}, I) , we need to solve the problem

$$\begin{aligned} \max_{\tilde{v}_i \in \mathbb{R}^p} \quad & \tilde{v}_i^T X^T X \tilde{v}_i, \quad i = 1, \dots, k \\ \text{s.t.} \quad & \tilde{v}_i^T S^{-1} \tilde{v}_i = 1, \quad i = 1, \dots, k \\ & \tilde{v}_i^T S^{-1} \tilde{v}_j = 0, \quad 1 \leq i < j \leq k \end{aligned} \tag{18}$$

For the principal axes on the triple (X, S, I) , we need to solve

$$\begin{aligned} \max_{v_i \in \mathbb{R}^p} \quad & v_i^T S X^T X S v_i, \quad i = 1, \dots, k \\ \text{s.t.} \quad & v_i^T S v_i = 1, \quad i = 1, \dots, k \\ & v_i^T S v_j = 0, \quad 1 \leq i < j \leq k \end{aligned} \quad (19)$$

Now if we make the change of variables $\tilde{v}_i = S v_i$, problems (18) and (19) are the same.

B Proof of Theorem 2

The proof here follows almost exactly from [Purdom \(2011\)](#), but I am including a full proof for completeness.

First some notation. For a weight vector w satisfying $w^T \mathbf{1} = 1$, let $P_w = I - \mathbf{1}w^T$ represent the weighted centering operator, and let D_w be the diagonal matrix with w along the diagonal. We have p variables measured on n samples. Let $C \in \mathbb{R}^{n \times p}$ be our original data matrix with C_{ij} containing the count of variable j for sample i , and let w_L and w_S denote sample and variable weights, respectively. These are obtained by normalizing the row sums and column sums, so $w_L = C\mathbf{1}/\mathbf{1}^T C\mathbf{1}$ and $w_S = C^T\mathbf{1}/\mathbf{1}^T C\mathbf{1}$. Let $X \in \mathbb{R}^{n \times p}$ be the matrix with frequency profiles for each sample, so $X = D_{w_L}^{-1}C$. Finally, let the matrix $\delta \in \mathbb{R}^{p \times p}$ contain the squared Euclidean distances between variables. We are assuming that these distances are Euclidean.

DPCoA

For the first step of DPCoA, we get the variable locations from classical multi-dimensional scaling. The weighted version of multi-dimensional scaling is obtained by finding the eigendecomposition of $D_{w_S}^{1/2} P_{w_S} (-\delta/2) P_{w_S}^T D_{w_S}^{1/2}$. Then we have

$$U \Lambda U^T = D_{w_S}^{1/2} P_{w_S} (-\delta/2) P_{w_S}^T D_{w_S}^{1/2} \quad (20)$$

$$Z = D_{w_S}^{-1/2} U \Lambda^{1/2} \quad (21)$$

$$Y = XZ \quad (22)$$

Z is then a matrix in $\mathbb{R}^{p \times d}$ (d the dimension of the space the points are embedded in, $d < p$) containing the coordinates of the variable points given by multi-dimensional scaling. Since the rows of X contain the frequencies of the variables at each location, the rows of Y contain the barycenters of the variable clouds corresponding to each sample.

The second step of DPCoA, now that we have the barycenters of each sample in Y , is to do PCA on the triple (Y, I, D_{w_L}) . This means we have to solve

$$Y^T D_{w_L} Y M = M \Lambda \quad M^T M = I \quad (23)$$

$$Y Y^T D_{w_L} L = L \Lambda \quad L^T D_{w_L} L = I \quad (24)$$

The sample scores are then found in $L\Lambda^{1/2}$ and the variable scores are found in ZM . We can rewrite the first equation in (24) as

$$L\Lambda = YY^T D_{w_L} L \quad (25)$$

$$= XZZ^T X^T D_{w_L} L \quad (26)$$

$$= X D_{w_S}^{-1/2} U \Lambda U^T D_{w_S}^{-1/2} X^T D_{w_L} L \quad (27)$$

$$= X P_{w_S}(-\delta/2) P_{w_S}^T X^T D_{w_L} L \quad (28)$$

Then since P_{w_S} is a projection operator, $P_{w_S} = P_{w_S} P_{w_S}$ and so the previous line can be rewritten as

$$L\Lambda = X P_{w_S}(-P_{w_S} \delta P_{w_S}^T / 2) P_{w_S}^T X^T D_{w_L} L \quad (29)$$

Generalized PCA

First of all, recall that since X is a contingency table, centering X by row and centering X by column are the same, $X P_{w_S} = P_{w_L}^T X$. Call this centered matrix \tilde{X} .

Now consider generalized PCA of the triple (\tilde{X}, Q, D_{w_L}) where \tilde{X} is a column-centered version of X , so $\tilde{X} = X P_{w_S}$ and $Q = P_{w_S}(-\delta/2) P_{w_S}^T$. The equations that need to be satisfied for this gPCA are

$$\tilde{X}^T D_{w_L} \tilde{X} Q A = A \Psi \quad A^T Q A = I \quad (30)$$

$$\tilde{X} Q \tilde{X}^T D_{w_L} B = B \Psi \quad B^T D_{w_L} B = I \quad (31)$$

$B\Psi^{1/2}$ contains the sample scores from the gPCA. By comparing line (31) and line (29), we see that the conditions for the pair B, Ψ and the pair L, Λ are the same, and so the sample scores from gPCA and DPCoA are the same up to a sign change.

Then the variable scores given by DPCoA are given by ZM . The generalized SVD tells us that $Y = L\Lambda^{1/2}M^T$, which, along with $M^T M = I$ and $L^T D_{w_L} L = I$ implies that $M^T = \Lambda^{-1/2} L^T D_{w_L} Y$. The generalized SVD of \tilde{X} is $\tilde{X} = B\Psi^{1/2}A^T$, which, along with the corresponding orthogonality conditions, implies that $\tilde{X} Q A \Psi^{-1} = B\Psi^{-1/2}$. Then we can rewrite the variable scores ZM as

$$ZM = ZY^T D_{w_L} L \Lambda^{-1/2} \quad (32)$$

$$= ZZ^T X^T D_{w_L} L \Lambda^{-1/2} \quad (33)$$

$$= D_{w_S}^{-1/2} U \Lambda U^T D_{w_S}^{-1/2} X^T D_{w_L} L \Lambda^{-1/2} \quad (34)$$

$$= P_{w_S}(-\delta/2) P_{w_S}^T X^T D_{w_L} B \Psi^{-1/2} \quad (35)$$

$$= Q \tilde{X}^T D_{w_L} B \Psi^{-1/2} \quad (36)$$

$$= Q \tilde{X}^T D_{w_L} \tilde{X} Q A \Psi^{-1} \quad (37)$$

$$= Q A \quad (38)$$

So we can get the variable scores from DPCoA by multiplying the variable scores from gPCA by Q .

References

- Allen, G. I., Grosenick, L., and Taylor, J. (2014). A generalized least-square matrix decomposition. *Journal of the American Statistical Association*, **109**(505), 145–159.
- Brenner, D. J., Staley, J. T., and Krieg, N. R. (2005). Classification of procaryotic organisms and the concept of bacterial speciation. In *Bergeys Manual of Systematic Bacteriology*, pages 27–32. Springer.
- Callahan, B. J., Sankaran, K., Fukuyama, J. A., McMurdie, P. J., and Holmes, S. P. (2016). Bioconductor workflow for microbiome data analysis: from raw reads to community analyses. *F1000Research*, **5**.
- Chang, Q., Luan, Y., and Sun, F. (2011). Variance adjusted weighted unifracs: a powerful beta diversity measure for comparing communities based on phylogeny. *BMC Bioinformatics*, **12**(1), 1.
- Chang, W., Cheng, J., Allaire, J., Xie, Y., and McPherson, J. (2016). *shiny: Web Application Framework for R*. R package version 0.13.2.
- Chen, J., Bittinger, K., Charlson, E. S., Hoffmann, C., Lewis, J., Wu, G. D., Collman, R. G., Bushman, F. D., and Li, H. (2012). Associating microbiome composition with environmental covariates using generalized unifracs distances. *Bioinformatics*, **28**(16), 2106–2113.
- Cohan, F. M. (2002). What are bacterial species? *Annual Reviews in Microbiology*, **56**(1), 457–487.
- Dethlefsen, L. and Relman, D. A. (2011). Incomplete recovery and individualized responses of the human distal gut microbiota to repeated antibiotic perturbation. *Proceedings of the National Academy of Sciences*, **108**(Supplement 1), 4554–4561.
- Doolittle, W. F. and Papke, R. T. (2006). Genomics and the bacterial species problem. *Genome Biology*, **7**(9), 1.
- Dray, S., Pavoine, S., and Aguirre de Cárcer, D. (2015). Considering external information to improve the phylogenetic comparison of microbial communities: a new approach based on constrained double principal coordinates analysis (cdpcoa). *Molecular Ecology Resources*, **15**(2), 242–249.
- Edgar, R. C. (2010). Search and clustering orders of magnitude faster than blast. *Bioinformatics*, **26**(19), 2460–2461.
- Holmes, S. (2008). Multivariate data analysis: the French way. *Probability and Statistics: Essays in Honor of David A. Freedman*. Institute of Mathematical Statistics, Beachwood, Ohio, pages 219–233.

- Johnstone, I. M. and Lu, A. Y. (2012). On consistency and sparsity for principal components analysis in high dimensions. *Journal of the American Statistical Association*.
- Kondor, R. I. and Lafferty, J. (2002). Diffusion kernels on graphs and other discrete structures. In *Proceedings of the 19th International Conference on Machine Learning*, pages 315–322.
- Li, C. and Li, H. (2008). Network-constrained regularization and variable selection for analysis of genomic data. *Bioinformatics*, **24**(9), 1175–1182.
- Lozupone, C. and Knight, R. (2005). Unifrac: a new phylogenetic method for comparing microbial communities. *Applied and Environmental Microbiology*, **71**(12), 8228–8235.
- Lozupone, C. A., Hamady, M., Kelley, S. T., and Knight, R. (2007). Quantitative and qualitative β diversity measures lead to different insights into factors that structure microbial communities. *Applied and Environmental Microbiology*, **73**(5), 1576–1585.
- Matsen, F. A. and Evans, S. N. (2013). Edge principal components and squash clustering: using the special structure of phylogenetic placement data for sample comparison. *PLoS ONE*.
- McMurdie, P. J. and Holmes, S. (2014). Waste not, want not: why rarefying microbiome data is inadmissible. *PLoS Comput Biol*, **10**(4), e1003531.
- Paradis, E., Claude, J., and Strimmer, K. (2004). APE: analyses of phylogenetics and evolution in R language. *Bioinformatics*, **20**, 289–290.
- Pavoine, S., Dufour, A.-B., and Chessel, D. (2004). From dissimilarities among species to dissimilarities among communities: a double principal coordinate analysis. *Journal of Theoretical Biology*, **228**(4), 523–537.
- Purdom, E. (2011). Analysis of a data matrix and a graph: Metagenomic data and the phylogenetic tree. *The Annals of Applied Statistics*, **5**(4), 2326–2358.
- Quast, C., Pruesse, E., Yilmaz, P., Gerken, J., Schweer, T., Yarza, P., Peplies, J., and Glöckner, F. O. (2013). The silva ribosomal rna gene database project: Improved data processing and web-based tools. *Nucleic Acids Research*, **41**(D1), D590–D596.
- Randolph, T. W., Zhao, S., Copeland, W., Hullar, M., and Shojaie, A. (2015). Kernel-penalized regression for analysis of microbiome data. *arXiv preprint arXiv:1511.00297*.
- Rapaport, F., Zinovyev, A., Dutreix, M., Barillot, E., and Vert, J.-P. (2007). Classification of microarray data using gene networks. *BMC Bioinformatics*, **8**(1), 35.

- Rinaldo, A. *et al.* (2009). Properties and refinements of the fused lasso. *The Annals of Statistics*, **37**(5B), 2922–2952.
- Shade, A. and Handelsman, J. (2012). Beyond the venn diagram: the hunt for a core microbiome. *Environmental Microbiology*, **14**(1), 4–12.
- Silverman, B. W. (1996). Smoothed functional principal components analysis by choice of norm. *The Annals of Statistics*, **24**(1), 1–24.
- Tibshirani, R. and Wang, P. (2008). Spatial smoothing and hot spot detection for cgh data using the fused lasso. *Biostatistics*, **9**(1), 18–29.
- Tibshirani, R., Saunders, M., Rosset, S., Zhu, J., and Knight, K. (2005). Sparsity and smoothness via the fused lasso. *Journal of the Royal Statistical Society: Series B (Statistical Methodology)*, **67**(1), 91–108.
- Witten, D. M., Tibshirani, R., and Hastie, T. (2009). A penalized matrix decomposition, with applications to sparse principal components and canonical correlation analysis. *Biostatistics*, **10**(3), 515–534.